Ice Lead Orientation Characteristics in the Winter Beaufort Sea

Glenn F. Cunningham 1, Ronald Kwok[1] and Jeff Banfield[2]

[1]Jet Propulsion Laboratory
California Institute of Ethnology
4800 Oak Grove Drive, Pasadena, CA 91109
T:818-354-8328 F:818-393-5285 EMail:glenn@malibu.jpl.nasa.gov

[2]Dept. of Mathematical Sciences
Montana State University
Bozeman, MT 59717

Abstract

The directional orientations of leads in the winter ice pack of the Beaufort Sea are studied both spatially and temporally. Data from the European Earth Resources Satellite-1 (ERS-1) Synthetic Aperture Radar (SAR) was used. The SAR data was produced in image form at the Alaska SAR Facility (ASF) with 100m x 100m pixel resolution. The lead ice pixels, which included all non-multiyear ice, were defined using a simple thresholding of the radar backscatter values. The orientations of the leads covering the Beaufort Sea during the period of January through March of 1992 were derived using a lead skeletonization technique. Results show a strong temporal persistence in the distribution and orientation of the leads during this period. The orientation of leads newly-formed within a 3-day period were then compared to both the local and large-scale ice deformation fields. Results show a consistent relationship between the orientations of the newly-formed leads and the principal direction of shear within the ice motion fields.

Introduction

The characterization of lead structures in the Arctic Ocean sea-ice cover has been made mostly through the use of visual imagery with limited spatial and temporal sampling, Barry et *al.* (1989) roughly mapped large scale lead features for one day in each of three consecutive years from DMSP visible imagery for comparison with geostrophic wind patterns. Marko and Thomson (1977) analyzed in detail an occurrence of lead-formation in relation to the local ice deformation field. In this study, we attempt to study lead orientation characteristics over the entire Beaufort Sea during a three-month period. This is possible through the use of ERS-1 SAR image data and automated techniques for determining lead orientations and both local and large-scale ice deformation fields.

This study was carried out in two parts. First, the basin-wide lead distribution was studied on the large scale both spatially and temporally. Second, the directional orientations of newly opened leads were compared to the principal direction of shear within both the local and large-scale ice motion fields.

Basin-wide Lead Orientations and Distribution

The Beaufort Sea was sampled with SAR imagery during January through March of 1992. Four time periods around day-of-year (doy) 17, 41, 66 and 88 were studied with from 82 to 93 images (100m x 100m pixel resolution) for each time period. Kwok and Cunningham (1994) showed that multi-year ice and first-year or younger ice can be distinguished using radar backscatter measurements. With this in mind, each SAR image was "classified" using a backscatter value of -14dB as a threshold, The ice with backscatter lower than the threshold was classified as lead ice for this study, which essentially includes all non-multiyear ice.

Each of the classified images was then analyzed using a lead skeletonization technique described in Banfield (1992). This skeletonization scheme determines a variety of parameters describing the characteristics of each lead in an image. A sample portion (~20km x 15km) of a classified image with results from the skeletonization analysis is seen in Figure 1. As shown by the white line segments, both straight leads and connected or branched lead segments are

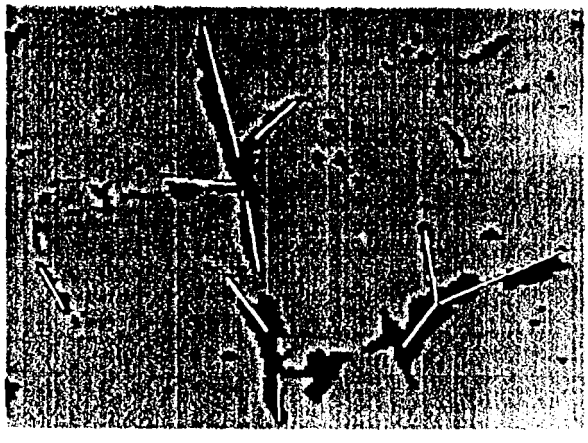

Figure 1. A subscene of a classified SAR image with results from the skeletonization analysis shown as white line segments.

included in the. results. After leads or lead segments with limited size or excessive curvature were filtered out, the orientations of the leads and lead segments were gathered into 10° directional bins.

The plots in Figures 2a-d summarize the lead population) for the region, The time span of the sampled SAR images is given at the top of each plot. The results from each SAR image arc represented by a cluster of lines plotted at the image center. Each line of a cluster has length relative to the number of leads or lead segments in its plotted direction bin. Some general characteristics of the lead populations arc readily observed. '1'here appears to be a rather sharp transition zone angling from (78.5°N,160°W) toward (76°N,120°W) delineating generally cast-west aligned leads to the north and north-south aligned leads in the south, The SAR images in this transition zone readily show a mixture of these two directional maxima. The southern field contains more leads with a larger variance in directional orientation. Also, there is little temporal change in these fields, except in Figure 2d where the northern half appears to contain more leads with a larger variance in directions.

These results seem to show a rather static lead population. Since this study was made during a period of limited large scale ice movement, ncw leads forming at this time arc possibly very thin and may not be sufficiently discerned by this classification scheme. Due to the threshold classification scheme, many of the leads identified in this dataset contain icc that may be days, weeks or even months old and therefore may not be responsive to the local deformation field. If these older, thicker leads sufficiently populate the data, the result ofa static field would not be surprising. For this reason, fur ther studies were made looking specifically ar newly - formed leads.

Newly.forn)cd Lead Orientations

The relationship between the orientations of ncw]y-opened leads and the local and large-scale deformation fields was studied. Pairs of SAR images taken 3 days apart were visually sampled to find newly-formed leads. A set of 37 pairs of SAR images containing these new leads was used. The orientations of the leads were measured and compared to both the local and large-scale deformation fields. These fields are characterized by the direction of the axis of

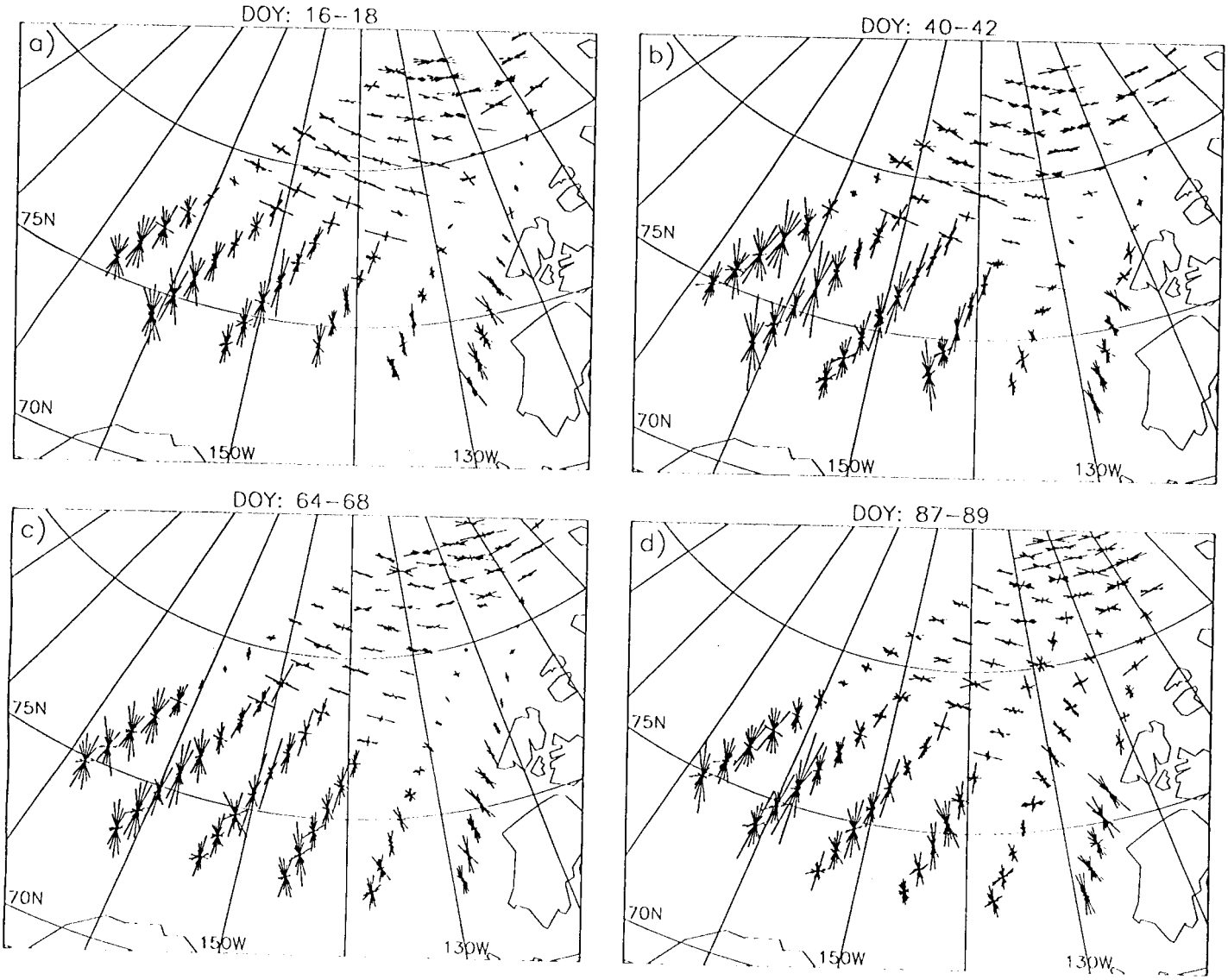

Figure 2. Results of the lead orientation sampling. The line clusters are centered at the SAR image locations a) DOY 16-18; b) DOY 40-42; c) DOY 64-68; d) DOY 87-89.

maximum stretching deformation, or the principal direction of shear. The scalar magnitude of the shear e is defined as:

$$e = \left[\left(\frac{\partial u}{\partial x} - \frac{\partial v}{\partial y}\right)^2 + \left(\frac{\partial u}{\partial y} + \frac{\partial v}{\partial x}\right)^2 \right]^{1/2}$$

while the principal direction of shear θ is defined as:

$$\theta = \frac{1}{2} \operatorname{atan}\left[\left(\frac{\partial u}{\partial y} + \frac{\partial v}{\partial x}\right) / \left(\frac{\partial u}{\partial x} - \frac{\partial v}{\partial y}\right) \right]$$

where u and v arc the ice velocity components in the x and y directions of a polar stereographic grid for the period between SAR images (3 days). Using the ice motion tracker described in Kwok *et al. (1990),* the local shear vector is calculated from the deformation of a regular grid of points spaced at 5km intervals covering the overlapping areas of the two SAR images. The large scale shear vector is calculated from daily large scale ice motion fields produced from surface pressure fields, ice buoy data and SAR ice motion data (Kwok and Colony, *in preparation).*

The shear vectors from the large and small scale ice motion fields arc compared in Figures 3a and 3b. The dashed lines show the least-squares fit corresponding to the correlation coefficient (r) and slope (m) values on the plots, The results show reasonably good agreement in both magnitude and direction, Also shown is the relationship between the lead direction and the corresponding principal direction of shear for both the large scale (Fig. 3c) and local (Fig. 3d) ice deformation fields. Here, the dashed lines show the mean value of the. angle differences. The data show consistent mean angle differences of 72.1° and 72.7° relative to bed] large scale and local ice motion, respectively.

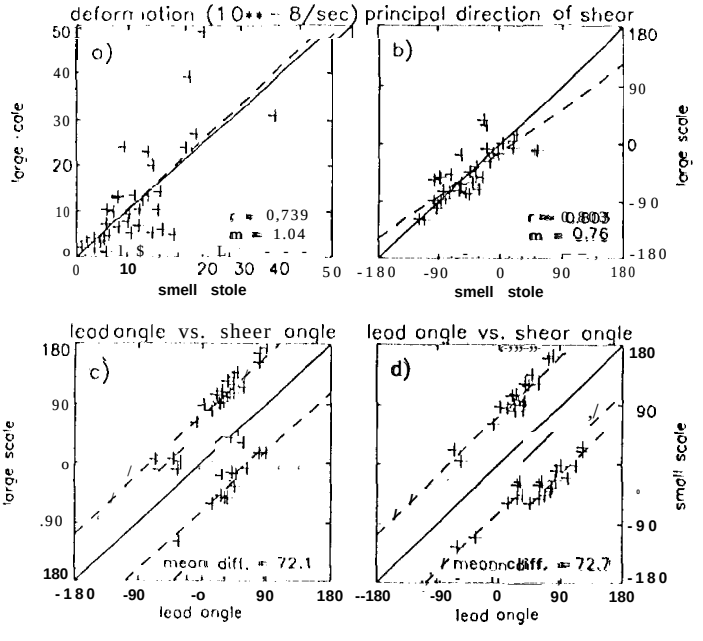

Figure 3. Comparisons of ice deformation angles and newly-formed lead orientations. a) Deformation magnitudes of large-scale versus local ice motion; b) Principal direction of shear for large-scale versus local ice motion; c) I&ad angle. versus large-scale principal direction of shear; d) Lead angle versus local principal direction of shear.

Conclusions

The first part of this study showed a persistent lead population over the winter Beaufort Sca in the first months of 1992. As previously mentioned, the leads classified here probably contain some thicker first-year ice formed during the fall transition and early winter months. Further work should be done to correlate the lead patterns to the overall ice stress patterns of the fall and early winter months.

The relationship between newly-formed lead angles and ice deformation parameters is consistent within the dataset described here. The study of Marko and Thomson (1977) found a lead forming at an angle of 14° to the major compression axis of the ice motion. Erlingsson (1988) summarized other studies with angles ranging from 14° to 16°. This study results in an angle between the lead and compression axis of 17° to 18°.

This study illustrates both the use of SAR imagery for lead characterization and the automation of directional comparisons with both large and small scale ice deformation. This work is preliminary in that the lead skeletonization scheme includes other lead parameters such as lead area and average width. Analysis of these additional lead parameters along with the use of a more robust lead classification scheme are areas for further work.

Acknowledgments

The research described in this paper was carried out by the Jet Propulsion Laboratory, California Institute of Technology, under a contract with the National Aeronautics and Space Administration,

References

Banfield, J. "Skeletal Modeling of Ice Leads." *IEEE Transactions on Geoscience and Remote Sensing 30 (1992):* pp. 918-923.

Barry, R. G., M.W. Miles, R.C. Cianflone, G. Scharfen and R.C. Schnell. "Characteristics of Arctic Sea Ice from Remote-Sensing Data and Their Relationship to Atmospheric Processes, " *Annals of Glaciology 12 (1989):* pp. 9-1 S.

Erlingsson, B. "Two-Dimensional Deformation Patterns in Sea Ice." *Journal of Glaciology 34 (1988):* pp. 301-308.

Kwok, R., J.C. Curlander, R. McConnell and S. Pang. "An Ice Motion Tracking System at the Alaska SAR Facility." *IEEE J. of Oceanic Engineering* 15 (1990): pp. 44-54.

Kwok, R. and G.F. Cunningham. "Backscatter Characteristics of the Winter Ice Cover in the Beaufort Sea." *J. of Geophysical Research 99(1994):* pp. 7787-7802.

Kwok, R. and R. Colony. "Large/Small Scale Ice Motion in the Pacific Sector of the Arctic Basin." in *preparation.*

Marko, J.R. and R.E. Thomson. "Rectilinear Leads and Internal Motions in the Pack Ice of the Western Arctic Ocean." *J. of* Geophysical *Research 82 (1977):* pp. 979-987.